

Analysis of double-diffusive convection with temperature modulations at the boundaries

Jayesh M. Mehta

Department of Mechanical Engineering, Illinois Institute of Technology, Chicago, IL, USA

The stability of a double-diffusive system modulated at both the boundaries is investigated. The modulations are found to cause mean flow, microconvection, at the edges of the diffusive core such that its amplitude dies off exponentially away from the boundaries. The mean heat and mass transfer values associated with microconvection are found to be several orders of magnitude less than those associated with diffusion, indicating the marginal influence of boundary modulations on scalar transport across the diffusive core. Linear stability analysis reveals that instability due to direct modes sets in earlier than predicted for nonperiodic boundaries. The critical thermal Rayleigh number correction factor associated with boundary modulations is found to be dependent on their amplitudes and the phase difference between them. This dependence is such that the convective currents have the largest amplitude when upper and lower modulations are in phase, resulting in the largest magnitude of the correction in critical thermal Rayleigh number.

Keywords: double-diffusive convection; solar ponds; linear stability analysis

Introduction

A fascinating feature of double-diffusive phenomena is the formation of a system of convecting layers separated by purely diffusive interfaces, although the system could be statically stable. In general, these layers are formed due to the influence of some external contributing factor (e.g., modulations at the boundaries) or are formed due to intrinsic instability arising from the destabilizing component. Figure 1 shows a photograph of double-diffusive layering observed during a laboratory experiment by Mehta (1985). During the experiment, a stably stratified salt water column was heated from the bottom. As can be seen, a three-layered system ensues where a lower mixed convecting layer forms underneath a stable diffusive core, with an interfacial boundary layer separating them. If the upper boundary of such a system is left open to ambient, then wind shear and evaporative cooling give rise to two additional layers: an upper mixed convecting layer and an upper interfacial boundary layer, e.g., in solar ponds.

The theory of double-diffusive convection is mathematically rich. For example, Huppert and Moore (1976) simulated double-diffusive convection in a small aspect ratio box through periodic, period doubling, chaotic, and steady regimes. Knobloch and Proctor (1981) investigated weakly nonlinear convection when the linear steady and oscillatory instabilities are both nearly marginal. Zangrando and Bertram (1984) investigated the linear stability of double-diffusive convection stabilized by a salinity gradient, with a minimum in the center

of the convecting layer. They concluded that the marginal stability curves for oscillatory modes are complex and typically exhibit both low and high wave number minima with respect to temperature gradient required to initiate convection. Bretherton (1985) further extended the results of Zangrando and Bertram (1984) and concluded that at low saline Rayleigh numbers the most unstable low wave number mode can also become the most unstable high wave number mode due to an existing loop or a kink in the marginal stability curve.

Witte and Newell (1985) used a thermal burst stability model as the basis for erosion/growth of the diffusive core predictions. They assumed diffusion at the boundary as the primary mechanism and ignored the influence of fluid behavior in the convecting zone. The diffusive core erosion (caused by ascending thermals from the heated bottom) model of Hull and Mehta (1987) was further extended by Hull and Katti (1987) to include the effects of the lower boundary undulation produced by thermal plumes. The undulation was characterized by indentation of the normally flat boundary above the plumes and depression of the boundary between the plumes. This refinement was found to yield a better understanding of the physical processes that cause diffusive core erosion.

In this study, we extend the analysis of Hull and Mehta (1987) in the following respects:

- This analysis includes the influence of descending thermal plumes on the diffusive core upper boundary also. The influence is such that due to thermal plumes, the upper boundary experiences temperature modulations of different amplitude and phase compared with those at the lower boundary. This extends and completes the study of Hull and Mehta (1987) such that it provides a physical understanding of mechanisms that cause five-layered stable double-diffusive systems, such as solar ponds.
- Secondly, a linear stability analysis is carried out to delineate the influence of boundary modulations on the instability caused by direct modes.

Address reprint requests to Dr. Mehta at his current address: Mail Drop A309, Combustion and Heat Transfer Technology, General Electric Aircraft Engines, Cincinnati, OH 45215, USA.

Received 19 December 1990; accepted 13 January 1992

© 1992 Butterworth-Heinemann

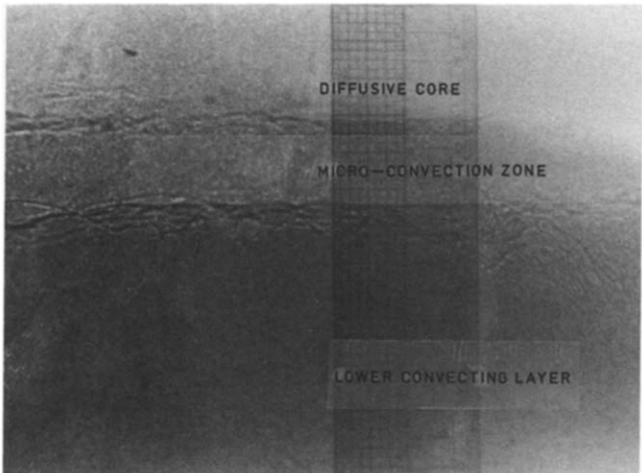


Figure 1 Photograph of the interface between the lower convective zone and the diffusive core

In addition, the analysis of Kelly and Pal (1976), is extended such that the effects of a second stabilizing diffusive component on singly diffusive convection are illustrated in this paper.

Mathematical model

The analysis is based on the premise that convective thermals in upper and lower convective zones impinge on diffusive core boundaries and produce a spatially periodic temperature distribution along the boundaries. The time scales of these modulations are assumed to be much larger than those for motion within the diffusive core. The salinity distribution at the boundaries is assumed to be uniform, and both the temperature and the salinity boundaries are assumed to be at the same vertical coordinate.

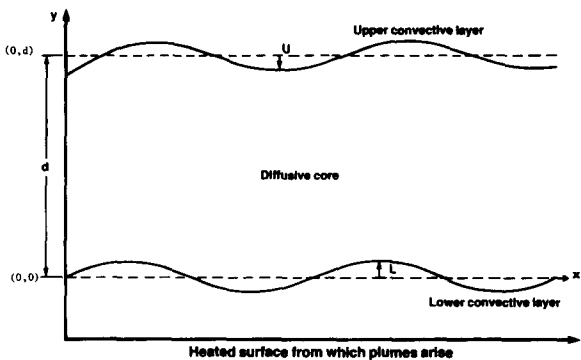


Figure 2 Schematic of the modeled thermohaline system

Figure 2 depicts a schematic of the investigated model. As shown, an infinitely long horizontal fluid slab is assumed bounded by two dynamically free boundaries at $y = 0$ and $y = d$. In addition, the boundaries are assumed to be perfect conductors of heat and solute, and the surface tension effects at the boundaries are neglected. We further assume that the fluid is incompressible, thermophysical properties are constant, convection is two-dimensional (2-D), and the Boussinesq approximation is valid. In addition, the modulations at lower and upper boundaries are assumed to have amplitudes L and U , respectively, such that $\max(L, U) \ll \delta$, where $\delta \ll 1$. It is also assumed that the upper temperature modulation lags behind the lower temperature modulation by a phase difference, β .

Although, some of the following mathematical steps are described fully by Mehta and Hull (1987), they are given here for continuity and completeness.

The upper boundary ($y = d$) and the lower boundary ($y = 0$) both have the temperature (T) and the salinity (S) fronts such that they are constant in time:

$$S(x, d) = 0, \quad T(x, d) = U \Delta T \sin k(x + \beta) \tag{1}$$

Notation

c_1	Arbitrary constant, Equation 36
c_2	Arbitrary constant, Equation 36
d	Height of the diffusive core
g	Acceleration due to gravity
k	Modulating wave number
k_c	Natural wave number associated with non-periodic free boundaries
k_d	Thermal conductivity of the fluid
k_s	Saline diffusivity
k_t	Thermal diffusivity
Nu	Mean Nusselt number
p	Equation 16a
Pr	Prandtl number
R_1	Correction in critical thermal Rayleigh number
R_{12}, R_{13}	$0(\epsilon)$ and $0(\epsilon^2)$ terms, Equation 25
R_s	Solutal Rayleigh number, $g\alpha_s\Delta Sd^3/\nu k_t$
R_t	Thermal Rayleigh number, $g\alpha_t\Delta Td^3/\nu k_t$
R_{tc}	Critical thermal Rayleigh number
R_p	Stability ratio, Rs/Rt
S	Local concentration
s_{12}, s_{13}	$0(\epsilon)$ and $0(\epsilon^2)$ terms, Equation 25
s_1	$0(1)$ term in concentration
s_2	$0(2)$ term in concentration

Sh	Mean Sherwood number
T	Local temperature
t_0	$0(0)$ term in temperature
t_1	$0(1)$ term in temperature
t_2	$0(2)$ term in temperature
t_{12}, t_{13}	$0(\epsilon)$ and $0(\epsilon^2)$ terms, Equation 25
u	x component of velocity

Greek symbols

α_s	Saline coefficient of expansion
α_t	Thermal coefficient of expansion
β	Relative phase difference between upper and lower modulations
γ	τ/R_p , Equation 16c
δ	Amplitude of temperature modulation
ΔT	Temperature difference across the core
ΔS	Salinity difference across the core
ϵ	Equation 36
Θ	A system of nonhomogeneous equations
Θ_0	A system of homogeneous equations
ν	Kinematic viscosity
ρ	Local density of fluid
τ	Ratio of diffusivities
ψ	Stream function

$$S(x, 0) = \Delta S, \quad T(X, 0) = \Delta T(1 + L \sin kx) \quad (2)$$

For 2-D convection, the governing equations are

$$k_s \nabla^2 S = u \frac{\partial S}{\partial x} + v \frac{\partial S}{\partial y} \quad (3)$$

$$k_t \nabla^2 T = u \frac{\partial T}{\partial x} + v \frac{\partial T}{\partial y} \quad (4)$$

$$\begin{aligned} \nabla^4 \Psi + \frac{g\alpha_s}{v} \frac{\partial S}{\partial x} - \frac{g\alpha_t}{v} \frac{\partial T}{\partial x} \\ = \frac{1}{v} \left[\frac{\partial \Psi}{\partial y} \left\{ \frac{\partial^3 \Psi}{\partial x \partial y^2} + \frac{\partial^3 \Psi}{\partial x^3} \right\} - \frac{\partial \Psi}{\partial x} \left\{ \frac{\partial^3 \Psi}{\partial y^3} + \frac{\partial^3 \Psi}{\partial y \partial x^2} \right\} \right] \end{aligned} \quad (5)$$

In the subsequent analysis, the following nondimensionizing scheme is used where the starred quantities are nondimensional variables.

$$\begin{aligned} \beta^* &= k\beta, & x^* &= \frac{kx}{d}, & y^* &= y/d, \\ T^* &= T/\Delta T, & S^* &= s/\Delta S, & \phi^* &= \psi/k_t \end{aligned} \quad (6)$$

Next, we expand the concentration, temperature, and stream function according to the following scheme where the asterisks are omitted for brevity.

$$(S, T, \phi, R_t) = \sum \delta^n (s_n, t_n, \phi_n, R_{tn}) \quad (7)$$

The above expansion scheme yields the basic diffusion solution for $n = 0$, such that it corresponds to nonmodulated stress-free boundaries. The solution is

$$s_0(x, y) = 1 - y, \quad \text{to } (x, y) = 1 - y, \quad \phi_0(x, y) = 0 \quad (8)$$

The stability of this configuration is widely studied, and it has been established that no convective currents for the fluid exist for $R_t < R_{tc}$, where R_{tc} is given by (e.g., Turner, 1979):

$$R_{tc} = (\tau + \text{Pr})R_s/(1 + \text{Pr}) + (1 + \tau)(1 + \tau/\text{Pr}) \left(\frac{27\pi^4}{4} \right) \quad (9)$$

The equations that govern $O(1)$, ($n = 1$) convection are

$$\nabla^2 s_1 + \frac{1}{k_s} \frac{\partial \phi_1}{\partial x} \cdot \frac{\partial s_0}{\partial y} = 0 \quad (10)$$

$$\nabla^2 t_1 + \frac{1}{k_t} \frac{\partial \phi_1}{\partial x} \cdot \frac{\partial t_0}{\partial y} = 0 \quad (11)$$

$$\nabla^4 \phi_1 + \frac{g\alpha_s}{v} \frac{\partial s_1}{\partial x} - \frac{g\alpha_t}{v} \frac{\partial \phi_1}{\partial x} = 0 \quad (12)$$

$$\text{at } y = 0, \quad t_1 = \sin(x), \quad s_1 = \frac{\partial^2 \phi_1}{\partial y^2} = \phi_1 = 0 \quad (13)$$

$$\text{at } y = 1, \quad t_1 = \sin(x + \beta), \quad s_1 = \frac{\partial^2 \phi_1}{\partial y^2} = \phi_1 = 0$$

Equations 10–12 demonstrate that at $O(1)$, the fluid motion in the double-diffusive slab is caused by the forcing at the boundaries. Since the forcing function is assumed to be periodic, we assume the final solution to be in the following form:

$$\begin{aligned} t_1(x, y) &= t_1(y) \sin x + t_u(y) \sin(x + \beta) \\ s_1(x, y) &= s_1(y) \sin x + s_u(y) \sin(x + \beta) \\ \phi_1(x, y) &= \theta_1(y) \cos x + \theta_u(y) \cos(x + \beta) \end{aligned} \quad (14)$$

where

$$\begin{aligned} t_1(y) &= \sum_{i=1}^4 a_i \frac{\sinh \lambda_i(1-y)}{\sinh \lambda_i}, & t_u(y) &= \sum_{i=5}^8 a_i \frac{\sinh \lambda_i y}{\sinh \lambda_i} \\ s_1(y) &= \sum_{i=1}^4 b_i \frac{\sinh \lambda_i(1-y)}{\sinh \lambda_i}, & s_u(y) &= \sum_{i=5}^8 b_i \frac{\sinh \lambda_i y}{\sinh \lambda_i} \\ \theta_1(y) &= \sum_{i=1}^4 c_i \frac{\sinh \lambda_i(1-y)}{\sinh \lambda_i}, & \theta_u(y) &= \sum_{i=5}^8 c_i \frac{\sinh \lambda_i y}{\sinh \lambda_i} \end{aligned} \quad (15)$$

The eigenvalues are given by

$$\begin{aligned} \lambda_1 &= -\lambda_5 = k \\ \lambda_2 &= -\lambda_6 = (p + k^2)^{1/2} \\ \lambda_3 &= -\lambda_7 = [k^2 + p/2(1 + i\sqrt{3})]^{1/2} \\ \lambda_4 &= -\lambda_8 = [k^2 - p/2(1 - i\sqrt{3})]^{1/2} \end{aligned} \quad (16)$$

The above set of equations provides a complete solution to Equations 10–12, with the boundary conditions 13, where p is given by

$$p = [k^2 R_t(1 - \gamma)/\gamma]^{1/3} \quad (16a)$$

In the above equations

$$R_p = \frac{\alpha_s \Delta S}{\alpha_t \Delta T}, \quad (16b)$$

and

$$\gamma = \tau/R_p \quad (16c)$$

The coefficients can be readily determined to be

for $\lambda_1 = k$, $c_1 = 0$, and

$$\begin{aligned} b_1 &= R_p a_1 \\ a_1 &= L/(1 - \gamma) \\ c_1 &= U/(1 - \gamma) \end{aligned} \quad (16d)$$

for $\lambda_i \neq k$

$$\begin{aligned} c_3 &= \frac{LP\gamma}{3k(1 - \gamma)}, & C_4 &= \frac{-LP\gamma(1 + i\sqrt{3})}{6k(1 - \gamma)} \\ c_5 &= \frac{-LP\gamma(1 - i\sqrt{3})}{6k(1 - \gamma)} \\ \text{and} \\ c_6 &= \frac{UP\gamma}{3k(1 - \gamma)}, & C_7 &= \frac{-P\gamma(1 + i\sqrt{3})U}{6k(1 - \gamma)} \\ c_8 &= \frac{-UP\gamma(1 - i\sqrt{3})}{6k(1 - \gamma)} \end{aligned} \quad (16e)$$

Also, the following relationship holds true:

for $\lambda_i \neq k$

$$\begin{aligned} a_i &= \frac{-kc_i}{(\lambda_i^2 - k^2)} & i &= 1, 2, \dots, 7, 8 \\ b_i &= \frac{(-k/\tau)c_i}{(\lambda_i^2 - k^2)} & i &= 1, 2, \dots, 7, 8 \end{aligned} \quad (16f)$$

The above set of equations provides a complete solution to Equations 10–12 with the boundary conditions 13.

Discussion of numerical results

The emphasis in the analysis is first to evaluate $O(1)$ mean flow results such that we can next calculate $O(2)$ mean quantities to yield mean heat transfer and mean mass transfer numbers.

Mean flow solutions

Equations 14–16 readily demonstrate that $O(1)$ solution is independent of Prandtl number of the fluid, and primarily depends on R_ρ , k , β , R_t and the amplitudes of the modulations. These effects are discussed in this section.

Figure 3 depicts $O(1)$ streamlines for $R_\rho = 0.011$. The calculations are performed for three different phase angles: 0.0 , $\pi/2$, and π . This has been done for $k = k_c$, the critical wave number for Rayleigh-Benard convection with stress-free boundaries. They also correspond to $R_t = 300$. As shown in the figure, for $\beta = 0^\circ$, closed cells appear with strongly vertical updrafts and downdrafts centered about the peak and valley of the boundary temperature modulations. At $\beta = \pi/2$ an accentuated tilt occurs in the cells that leads to non-zero local Reynolds stresses. The tilt also gives rise to local mean flow at $O(2)$ solutions. At $\beta = \pi$, the stress-free boundary conditions no longer can accommodate a single-tier structure of cells, and a two-tier structure appears that has two counterrotating cells positioned one on top of the other. A similar observation was made by Kelly and Pal (1978), who studied only the singly diffusive thermal convection with spatially periodic boundaries ($R_\rho = 0.0$).

Figures 4 and 5 show $O(1)$ streamlines for $R_\rho = 2.0$ and $R_\rho = 10.0$, respectively. They demonstrate the influence of the second diffusive component on $O(1)$ solution. As shown in Figure 4, at $\beta = 0$, a three-tier structure for the convection cells exists for $R_\rho = 2.0$. Unlike pure or nearly thermal convection (Figure 3), one row each of convection cells exist at the top and at the bottom boundary that corresponds to peak and valley of temperature modulations, and in addition a single counterrotating cell exists in the centre that has much lower circulation strength. What seems to have happened is that at $R_t = 300$ and $R_\rho = 2.0$, the thermal potential across the double-diffusive core is just not sufficient to support a single-tier convection cell that spans the full height of the core. In fact, as the streamline for $\beta = \pi/2$ and $\beta = \pi$ demonstrates, the influence of the second stabilizing diffusing component has been to shift lower and upper boundaries into the diffusive core such that the outer convecting cells now provide temperature modulations at the boundaries of the inner diffusive core. For

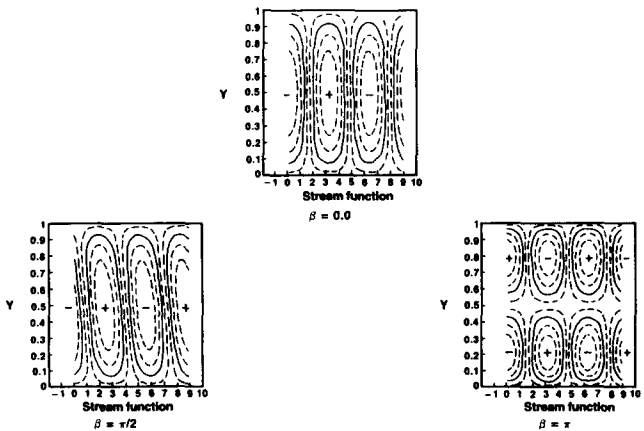


Figure 3 Streamlines of $O(\delta)$ convection cells ($R_\rho = 0.011$, $R_t = 300$, $k = k_c = 2.221$)

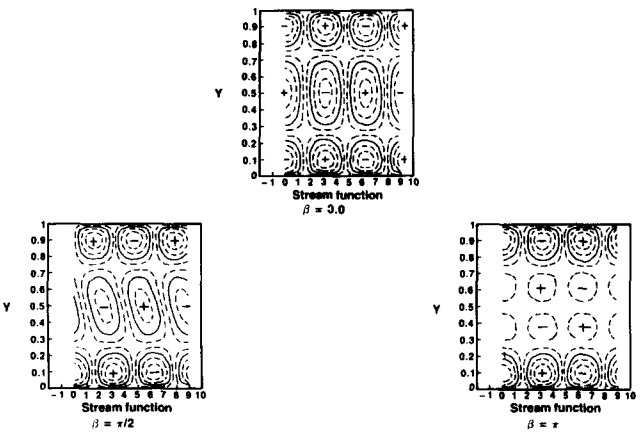


Figure 4 Streamlines of $O(\delta)$ convection cells ($R_\rho = 2.0$, $R_t = 300$, $k = k_c = 2.221$)

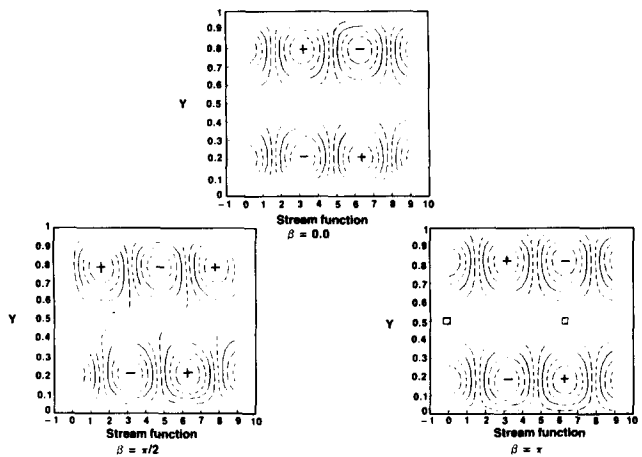


Figure 5 Streamlines of $O(\delta)$ convection cells ($R_\rho = 10.0$, $R_t = 300$, $k = k_c = 2.221$)

example, the influence of β , at $\beta = \pi/2$, now is to tilt only the middle tier convection cells that break off into an additional pair of counterrotating cells at $\beta = \pi$. As R_ρ is increased further (Figure 5), the stabilizing diffusing component is seen to play a dominant role. As shown, the thermal potential across the diffusive core is found to be sufficient to cause convection only at the edges. No convective cells appear in the middle of the fluid slab. However, at $\beta = \pi/2$ there is a slight tilt in the cells, which break off completely at $\beta = \pi$, resulting in a mild convection in the center.

The influence of increasing R_t is interesting. Figure 6 shows the streamlines for $R_t = 3 \times 10^8$ and $R_\rho = 10.0$. They also correspond to $k = k_c$. As can be seen, a four-tier structure occurs readily at $\beta = 0$, and the influence of the phase angle β is to only increase the circulation strengths of the inner convecting cells.

The results of Figures 3–6 lead to some interesting observations. First, Figure 3 shows that for a nearly thermal case, convection occurs for any value of R_t , due to modulations at the boundaries. This ought to result in higher heat and mass transfer values across the diffusive core than the transport values via pure diffusion only. However, as shown in Figures 4–6 the influence of the second diffusing component is to suppress convection and limit it to boundaries only. In particular, Figure 6 shows that at $R_\rho = 10$ and $R_t = 3 \times 10^8$, the convection is limited to only about 35 percent of the depth

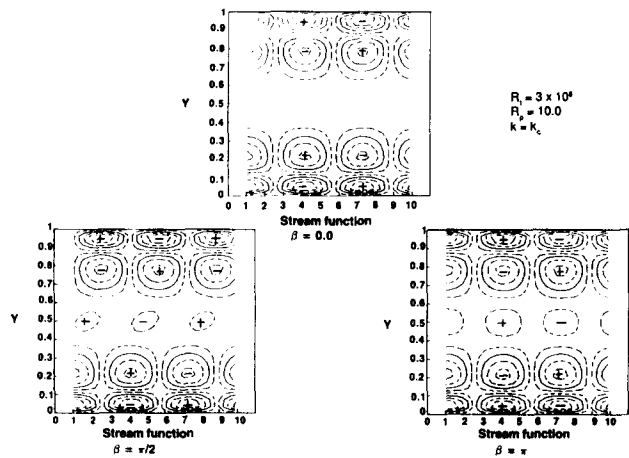


Figure 6 Streamlines of $O(\delta)$ convection cells ($R_p = 10.0$, $R_t = 3.0 \cdot 10^8$, $k = k_c = 2.221$)

at both the boundaries. This leads to the observation that at these conditions, a primary mode of heat and mass transports across the diffusive core is that of diffusion only.

Asymptotic results

As described earlier, Kelly and Pal (1976) studied the thermal convection problem and found that cells form either a single- or a double-tier structure that fills the entire fluid slab. In contrast to that study, the present analysis indicates that for a double-diffusive fluid the presence of the second diffusing component causes multilayering.

From Equations 14–16, the x -component of the mean velocity at the lower boundary is given by

$$u = -(k_t/d) \left[\frac{\lambda_2 c_2 \cosh \lambda_2 (1-y)}{\sinh \lambda_2} + \frac{\lambda_3 c_3 \cosh \lambda_3 (1-y)}{\sinh \lambda_3} + \frac{\lambda_4 c_4 \cosh \lambda_4 (1-y)}{\sinh \lambda_4} \right] \tag{17}$$

Here, we consider the effect of lower boundary modulation only, since the effect of upper boundary modulation will be symmetrical.

For large p the above equation reduces to

$$u = (-k_t/d) \frac{L\gamma^{3/2}\sqrt{R_t}}{3d} - [e^{-xy} - 2e^{-0.5xy} \cos(0.87xy)] \tag{18}$$

where $x = \sqrt{P}$.

As can be seen from Equation 18, the u velocity has the largest value at $y = 0$, and it decreases with increasing distance from the edges of the diffusive core. Furthermore, the vertical height of the convection cell is given by

$$\lambda_y = \frac{7.22}{\sqrt{P}} d \tag{19}$$

Recall that p is given by Equation 16a and it depends on the horizontal wave number k or the horizontal wavelength λ of the temperature modulation. Table 1 shows the variation of λ_y with the horizontal wave number k . These results are for $R_p = 15$ and $R_t = 10^{10}$. For the given example, vertical dimensions of the convection cell vary from about 2.69 cm for $k = 5$ to 0.365 cm for $k = 2,000$. These results also explain the multilayering phenomenon observed at the boundary between the lower convection layer and the diffusive core (Figure 1).

Mean $O(2)$ results

The $O(2)$ effects in terms of mean heat transfer and mass transfer across the diffusive core are determined next. At $O(2)$, the mean temperature and salinity distributions are given by

$$\begin{aligned} k^2 \frac{\partial^2 t_2}{\partial x^2} + \frac{\partial^2 t_2}{\partial y^2} - k \frac{\partial \phi_2}{\partial x} &= k \left[\frac{\partial \phi_1}{\partial y} \frac{\partial t_1}{\partial x} \frac{\partial \phi_1}{\partial x} \frac{\partial t_1}{\partial y} \right] \\ k^2 \frac{\partial^2 s_2}{\partial x^2} + \frac{\partial^2 s_2}{\partial y^2} - \frac{k}{\tau} \frac{\partial \phi_2}{\partial x} &= \frac{k}{\tau} \left[\frac{\partial \phi_1}{\partial y} \frac{\partial s_1}{\partial x} - \frac{\partial \phi_1}{\partial x} \frac{\partial s_1}{\partial y} \right] \end{aligned} \tag{20}$$

In the above equations, the right-hand side represents the $O(1)$ solution as evaluated above. Taking an average over a wavelength in x -direction:

$$\frac{d^2 t_2}{dy^2} = \frac{k}{2} \left[\frac{\partial \phi_1}{\partial y} \frac{\partial t_1}{\partial x} - \frac{\partial \phi_1}{\partial x} \frac{\partial t_1}{\partial y} \right] \tag{21}$$

and

$$\frac{d^2 s_2}{dy^2} = \frac{-k}{2\tau} \left[\frac{\partial \phi_1}{\partial y} \frac{\partial s_1}{\partial x} - \frac{\partial \phi_1}{\partial x} \frac{\partial s_1}{\partial y} \right] \tag{22}$$

The mean heat transfer to the fluid slab at the lower boundary is

$$\bar{Q}(0) = \frac{-k_d dT}{d} \Big|_{y=0} = \frac{k_d \Delta T}{d} \left[1 - \delta^2 \frac{dt_2}{dy} \Big|_{y=0} + \dots \right] \tag{23}$$

To $O(2)$ the mean Nusselt number is

$$\overline{Nu} = 1 - \delta^2 \frac{dt_2}{dy} \Big|_{y=0} \tag{23a}$$

Similarly, the mean Sherwood number is

$$\overline{Sh} = 1 - \delta^2 \frac{ds_2}{dy} \Big|_{y=0} \tag{24}$$

Figures 7 and 8 show the variation of mean Nusselt and Sherwood numbers with R_p , respectively. The thermal Rayleigh number R_t is chosen as a varying parameter in both the cases. These computations correspond to $\beta = 0$ case, where transport values were found to be at their maximum. Also, recall that $\overline{Nu} = 1$ and $\overline{Sh} = 1$ correspond to heat and mass transports via diffusion only. As the figures show, the transport values are negligibly small compared to diffusion. It can be readily concluded that in spite of boundary modulations, primary mode of heat and mass transports across the diffusive core is that of diffusion only.

Linear stability analysis

As demonstrated in the previous section, there is no critical thermal Rayleigh number for the double-diffusive problem with periodically varying boundaries. Convection occurs spontaneously for every value of R_t . However, as the present analysis deals with the boundary modulation resonance and its effect

Table 1 Size of typical convective cells within the microconvection zone ($R_p = 15$, $R_t = 10^{10}$)

k_x	λ	λ_y
5	1.21 m	2.69 cm
50	13.0 cm	1.25 cm
100	6.0 cm	0.991 cm
1000	1.0 cm	0.460 cm
2000	0.31 cm	0.365 cm

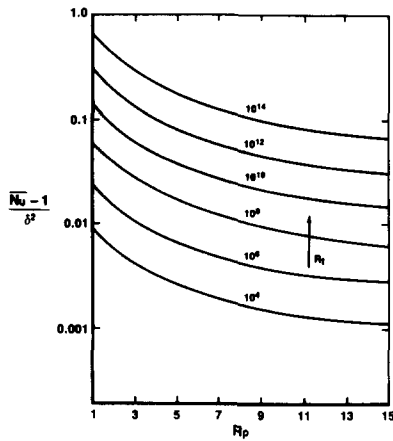


Figure 7 Mean Nusselt number variation with the stability ratio

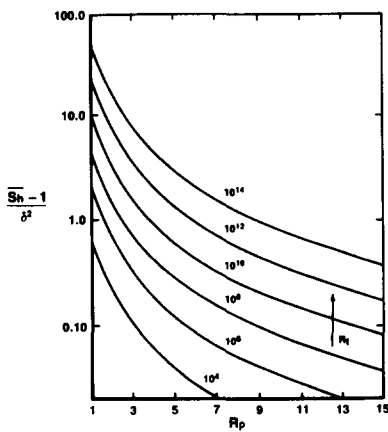


Figure 8 Mean Sherwood number variation with the stability ratio

on convection as $R_t \rightarrow R_{tc}$, R_{tc} is taken as that critical thermal Rayleigh number that corresponds to the case of double-diffusive convection with free upper and lower surfaces. In addition, the critical wave number k_c will also correspond to the above condition.

If the effects of boundary modulations are to be included in the solution to Equations 3–5, then R_{tc} is no longer an eigenvalue but depends on R_s , ratio of diffusivities τ , and the amplitude ε to be defined later. If the effects of boundary variations are small and if R_{tc} is the eigenvalue for nonperiodic boundary conditions, then

$$\begin{aligned} R_t &= R_{tc} + \varepsilon R_{12} + \varepsilon^2 R_{13} + \dots \\ s_1 &= \varepsilon s_{12} + \varepsilon^2 s_{13} + \dots \\ t_1 &= \varepsilon t_{12} + \varepsilon^2 t_{13} + \dots \\ \phi_1 &= \varepsilon \phi_{12} + \varepsilon^2 \phi_{13} + \dots \end{aligned} \quad (25)$$

In the above equations, $\varepsilon < \delta < \max(L, U)$ and will be defined later. R_{12} is the correction in the critical thermal Rayleigh number R_{tc} , which will account for effects of boundary modulations. The above expansion scheme yields, in addition to Equation 20

$$\nabla^4 \phi_2 + \frac{k}{Pr} \left[R_s \frac{\partial s_2}{\partial x} - R_{tc} \frac{\partial \phi_2}{\partial x} \right] = \frac{k R_{12}}{Pr} \frac{\partial t_1}{\partial x} + \frac{I}{Pr} \quad (26)$$

where

$$\begin{aligned} I_1 &= -k \left[\frac{\partial \phi_1}{\partial x} \cdot \frac{\partial^3 \phi_2}{\partial y^3} - \frac{\partial \phi_1}{\partial y} \cdot \frac{\partial^3 \phi_2}{\partial x \partial y^2} \right. \\ &\quad \left. + \frac{\partial \phi_1}{\partial x} \cdot \frac{\partial^3 \phi_2}{\partial x^2 \partial y} - \frac{\partial \phi_1}{\partial y} \cdot \frac{\partial^3 \phi_1}{\partial x^3} \right] \end{aligned} \quad (27)$$

The subscript 1 denotes the mean flow solution as obtained in the previous section. The boundary conditions that apply to above equations are

$$\begin{aligned} t_2 \sim s_2 \sim \phi_2 \sim \frac{\partial \phi_2}{\partial y} &= 0 \quad y = 0 \\ t_2 \sim s_2 \sim \phi_2 \sim \frac{\partial \phi_2}{\partial y} &= 0 \quad y = 1 \end{aligned} \quad (28)$$

In the present analysis, we are interested in the correction to R_{tc} , solution R_{12} . And it is obtained by invoking the solvability condition. For a system of nonhomogeneous equations

$$L(\Theta) = A(y) \quad (29)$$

that has the adjoint such that

$$L_{adj}(\Theta_0) = 0 \quad (30)$$

then the solvability condition requires that

$$\langle \Theta_0(y), A(y) \rangle = 0 \quad (31)$$

where $\langle \rangle$ denotes a linear product of the functions $A(y)$ and $\Theta_0(y)$.

Applying the above condition to Equations 26 and 27, it can be shown that if all of the nonlinear terms are neglected, then R_{12} is identically zero. In other words, the correction to R_{tc} is required only when variations at the boundaries cause mean flow in the diffusive core. Furthermore, from the solvability condition, it can be shown that the nonlinear terms on the right-hand side of Equations 26 and 27 amplify the natural disturbance with the wave number k_c only if

$$k_c = k/2 \quad (32)$$

and for all other values of the modulating wave numbers k , detuning will occur and the effect of boundary variations will die out. If we let

$$\begin{aligned} t_{12}(x, y) &= P_1(y) e^{i(2kx)} + P_1(y^*) e^{-i(2kx)} \\ s_{12}(x, y) &= P_2(y) e^{i(2kx)} + P_2(y^*) e^{-i(2kx)} \\ \phi_{12}(x, y) &= P_3(y) e^{i(2kx)} + P_3(y^*) e^{-i(2kx)} \end{aligned} \quad (33)$$

where the asterisks denote the conjugate pairs such that they satisfy Equations 20–27. Substitution of Equation 14 into Equations 20–26 leads to

$$\begin{aligned} (D^2 - 4k^2) P_1(y) - \frac{ik}{2} P_3(y) &= \frac{k}{4i} DF_1(y) + \frac{k}{2} DF_3(y) \\ (D^2 - 4k^2) P_2(y) - \frac{ik}{2} P_3(y) &= \frac{-k}{4i\tau} DF_2(y) + \frac{k}{2\tau} DF_3(y) \\ (D^2 - 4k^2)^2 P_3(y) - \frac{ik}{2Pr} R_{tc} P_1(y) + \frac{ik}{2Pr} R_s P_2(y) \\ &= k R_{12} + \frac{ikD^3}{4Pr} F_3(y) \end{aligned} \quad (34)$$

where F_1 , F_2 and F_3 are the functions of mean solutions as obtained in the previous section. These functions are fully given by Mehta (1985). If $R_t < R_{tc}$, a solution to above equations can be obtained by numerical integration. However, as $R_t \rightarrow R_{tc}$, the solution to R_{12} is obtained by invoking the solvability

condition. Let $P_{10}(y)$, $P_{20}(y)$, and $P_{30}(y)$ be the solution to the adjoint homogeneous boundary conditions, then the orthogonality condition dictates that

$$\int_0^1 P_{10}(y) \left\{ \frac{DF_1(y)k}{4i} + \frac{k}{2} DF_3(y) \right\} dy - \int_0^1 \frac{P_{20}(y)}{\tau} \left\{ \frac{DF_2(y)k}{4i} + \frac{k}{2} DF_3(y) \right\} dy + \int_0^1 P_{30}(y) \left\{ \frac{R_{12} + D^3 F_3(y)}{4Pr} \right\} dy = 0 \tag{35}$$

A solution to the above equation determines the correction factor R_{12} .

Discussion of stability analysis results

Baines and Gill (1969) have shown that for a double-diffusive fluid, first occurrence of instability can take the form of oscillations rather than direct convection if the component with smaller diffusivity is stably stratified, and Rs (that provides a dimensionless measure of stratification) is sufficiently large.

Figure 9 shows the influence of boundary modulations on R_{ic} . These computations correspond to upper surface modulation of 3 percent (while the lower surface modulation is varied from 0.50–3 percent). Two sets of computations, one corresponding to $\beta = 0$ and the other corresponding to $\beta = \pi$ are shown. As the figure shows, the influence of surface modulations is such that they reduce the critical thermal Rayleigh number. As the amplitude L of the modulations is increased, the correction factor R_{12} also increases, resulting in a lowered value of the critical thermal Rayleigh number.

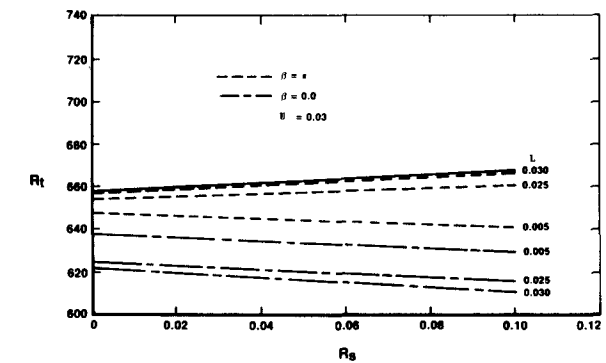


Figure 9 Stability boundaries for a double-diffusive system with periodic boundaries

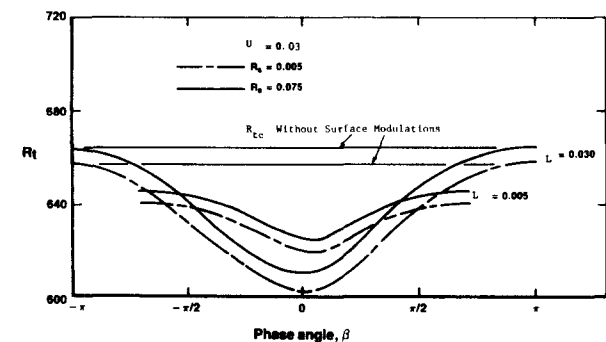


Figure 10 Variation of critical thermal Rayleigh number with the phase angle

The influence of the phase difference β is interesting. As shown in Figure 10, at $\beta = 0$ the correction factor R_{12} is found to have a larger value than at $\beta = \pi$. Figure 10 depicts the variation of the critical thermal Rayleigh number with the phase β . As can be seen, the correction factor R_{12} is found to have a maximum value at $\beta = 0$ and a minimum for $\beta = \pi$. This can be due to the following: In thermohaline convection the vertical temperature gradient is proportional to the lowest order motion induced by the horizontal temperature modulation via the baroclinic effect. If pressure is approximated by the hydrostatic pressure, then the vorticity generated by the above mechanism is proportional to $\nabla P \times \nabla T$. When this product has the same sign at the boundaries and through most of the vertical section, the induced flow will be the greatest and affect stability the most. For the Boussinesq fluid, ∇P is nearly a constant vector pointing downward, hence $\partial T / \partial X$ must have the same sign over the range of y (including the boundaries) in order to maximize $\partial T / \partial y$, i.e., the temperature modulations should be in phase at the boundaries as the analysis shows.

Now what remains to be established is the magnitude of the amplitude ε , as defined in Equation 25. The above analysis establishes the following:

- As $R_i \rightarrow R_{ic}$, the nonlinear effects must be included in the analysis.
- Furthermore, resonance occurs only if $k_c = k/2$. For any other values of k , detuning occurs and the influence of boundary modulations dies out.

Consequently, as suggested by Kelly and Pal (1976), the amplitude follows the following relationship for $c_2 \neq 0$.

$$\varepsilon^2 = \{ (R_i - R_{ic}) / R_{ic} \cdot c_2 \} + \delta c \tag{36}$$

where $c_1 \neq \delta \neq 0$. That is as $R_i \rightarrow R_{ic}$, the amplitude of disturbance that leads to instability (ε) is of the order of $\delta^{1/2}$, where order of δ is determined by the thermal boundary-layer thickness at the lower or upper heated surface, temperature difference across the diffusive core, and the thickness of the lower or upper convective zone, as described by Hull and Mehta (1987).

Conclusions

The stability of a double-diffusive system with periodic boundary conditions is investigated. The mean flow results reveal the following.

- The induced flow is a strong function of R_ρ and the mean quantities drop sharply with increase in stability ratio.
- Unlike pure thermal case, the convection cells do not fill the entire fluid slab for double-diffusive convection. At the edges of the diffusive core, $y = 0$ and $y = 1$, a multitude of shapes and sizes of the convection cells exist that depend on k .
- In spite of the presence of convection currents at the boundaries, the primary mode of heat and mass transport processes across the diffusive core is found to be that of diffusion. The corresponding Nusselt and Sherwood numbers are found to be strong functions of R_ρ , the modulating wave number k , and the phase difference β between the upper and the lower modulations. The latter influence is such that the Nusselt and the Sherwood numbers have the largest magnitude when both the modulations are in phase ($\beta = 0$).

The linear stability analysis reveals the following:

- The correction in the thermal Rayleigh number due to periodic boundaries is such that at low Rs instability due to direct modes sets in at a lower thermal Rayleigh number

than given by Equation 9. Furthermore, the correction is identically zero in the absence of the induced mean flow or for the nonresonant case when $k_c \neq k/2$.

- The correction due to boundary modulations is a strong function of the modulation amplitudes and the phase difference between them. The latter effect is such that the correction is largest when both the modulations are in phase ($\beta = 0$).

Acknowledgments

Parts of this work were submitted by the author toward fulfillment of the requirements for a Ph.D. degree. The author would like to thank Drs. S. Rosenblat and S. Nair of IIT for many stimulating discussions during the course of this study. Dr. John Hull of Argonne National Laboratory is acknowledged for his many valuable contributions to this study. The author would also like to acknowledge excellent typing by Mary Jo Schmees.

References

- Baines, P. G. and Gill, A. E. 1969. On the thermohaline convection with linear gradients. *J. Fluid. Mech.* **37**, 189
- Bretherton, C. S. 1985. A simplified theory of double diffusive convection in variable gradients. *Double Diffusive Motions*, The Joint ASCE/ASME Conference Proceedings
- Hull, J. R. and Katti, F. 1987. Microconvection effects of gradient zone boundaries. *Proc. Am. Solar Energy Society*, Portland, OR, USA, 493–497
- Hull, J. R. and Mehta, J. M. 1987. Physical model of gradient zone erosion in thermohaline systems. *Int. J. Heat Mass Transfer* **30**, 1027–1036
- Huppert, H. E. and Moore, D. R. 1976. Nonlinear double-diffusive convection. *J. Fluid Mech.* **58**, 821–854
- Kelly, R. E. and Pal, D. 1976. Thermal convection induced between non-uniformly heated horizontal surfaces. *Proc. 1976 Heat and Fluid Mech. Inst.*, vol. 2, Stanford University, Stanford, CA, USA
- Kelly, R. E. and Pal, D. 1978. Thermal convection with spatially periodic boundary conditions. *J. Fluid Mech.* **86**, 629–642
- Knobloch, E. and Proctor, M. R. E. 1981. Nonlinear periodic convection in double-diffusive systems. *J. Fluid Mech.* **108**, 291–316
- Mehta, J. M. 1985. Experimental and analytical investigation of a thermohaline double diffusive system. Ph.D. diss., I.I.T., Chicago, IL, USA
- Turner, J. S. 1979. *Buoyancy Effects in Fluids*. Cambridge Press, UK
- Witte, M. J. and Newell, T. A. 1985. A thermal burst model for the prediction of erosion and growth rate of a diffusive interface. *ASME*, Paper no. 85-HT-31
- Zangrando, F. and Bertram, L. 1984. Doubly diffusive linear stability with nonconstant gradients. Solar Energy Research Institute, Denver, SERI/TR 13825